

Coarse Grained Simulations of the Electrolytes at the Water–Air Interface from Many Body Dissipative Particle Dynamics

Aziz Ghoufi^{*,†} and Patrice Malfreyt[‡]

[†]Institut de Physique de Rennes, CNRS, UMR 6251, 263 avenue Général Leclerc, 35042 Rennes, France

[‡]Laboratoire de Thermodynamique et Interactions Moléculaires, CNRS, UMR 6272, LTIM, BP 10448, F-63000 Clermont-Ferrand, France

S Supporting Information

ABSTRACT: Modeling interfacial properties is a major challenge for mesoscopic simulation methods. Many-body dissipative particle dynamics (MDPD) is then a promising method to model heterogeneous systems at long time and length scales. However no rule exists to obtain a set of MDPD parameters capable to reproduce the thermodynamic properties of a molecular system of a specific chemistry. In this letter, we provide a general multiscale method to obtain a set of parameters from atomistic simulations using Flory–Huggins theory (FH) to be used with dissipative particle dynamics. We demonstrate the high quality and the transferability of the resulting parameters on the salt concentration dependence of surface tension. We also show the specificity of inorganic salt at the water–air interface. Our results indicate that the increase of surface tension with the salt concentration cannot be explained in terms of the charge image concept based on the Wagner, Onsager, and Samaras theory but rather in terms of the ion hydration.

The knowledge of structural and thermodynamic aspects of aqueous interfaces is a key element for various applications, such as energy saving, gas storage, and health. The most important of these interfacial properties is the surface tension (γ) driving the mass transport across the surface. While the modeling of heterogeneous systems and the computation of γ are well established from molecular simulation, the situation is less trivial at the mesoscopic scale. The dissipative particle dynamics method (DPD), introduced by Hoogerbrugge and Koelman¹ in 1992, is probably one of the most commonly used methods to reach the mesoscopic scale. The main advantage of this method is that it gives access to longer time and length scales than those used in conventional MD simulations.

The recent introduction of many-body interactions in DPD (MDPD),^{2,3} opens the way of modeling heterogeneous systems.^{4–6} Recently, a water DPD set of parameters has been developed⁵ to model complex interfacial aqueous systems. Unfortunately, unlike the usual DPD, no procedure can provide a realistic set of MDPD parameters. We shall provide a theoretical route to compute the MDPD interparticles force field from a multiscale approach by combining the Flory–Huggins (FH) theory and atomistic simulations. We focus here on the specificity of salt solutions on the water–air interface.

It is now well-established that most inorganic salts (NaCl, NaF, NaBr, NaI) increase the surface tension of water and present a negative adsorption at the Gibbs equimolar dividing surface (GDS).^{7–12} From 1924, several experimental,^{13–16} theoretical,^{8,9,17} and computational^{10–12} works have been carried out to highlight the microscopic processes involving the increase of γ . The change in the surface tension has been interpreted by Wagner, Onsager, and Samaras (WOS)¹⁷ in terms of a depletion of the salt molecules at the interface. Actually, ions approaching the water–air interface see their

image charge leading to a repel in the bulk phase. This produces a depletion boundary near to the interface which can be related to the excess surface tension. It is then very challenging to use the MDPD methods with the explicit/implicit incorporation of electrostatics interactions to model and understand the salt effect on the surface tension at the mesoscopic scale. These fundamental questions can be addressed here: (i) Are the electrostatic interactions required to model the dependence of the surface tension on the salt concentration at a mesoscopic scale?; (ii) is it possible to develop an effective set of parameters based upon the FH theory transferable to the surface tension?; (iii) are the cross-interactions fundamental to model the salt solutions at the liquid–vapor interface?; and (iv) are the mesoscopic models in line with the recent coarse grained theory of the ion hydration?

THEORETICAL BACKGROUND

In the standard DPD method,¹ particles interact with the force \mathbf{f}_i defined as the sum of three contributions $\mathbf{f}_i = \sum_{j \neq i} (\mathbf{f}_{ij}^C + \mathbf{f}_{ij}^R + \mathbf{f}_{ij}^D)$, where the random \mathbf{f}_{ij}^R and dissipative \mathbf{f}_{ij}^D force are pairwise and additive. Within the many body DPD technique, the conservative force^{2,3,18,19} is not only dependent on the interparticle separation but also on the local particle density. The resulting conservative force is then expressed as

$$\mathbf{f}_{ij}^C = a_{ij}\omega_C(r_{ij})\mathbf{e}_{ij} + b_{ij}[\bar{\rho}_i + \bar{\rho}_j]\omega_d(r_{ij})\mathbf{e}_{ij} \quad (1)$$

where the first term of eq 1 represents an attractive interaction ($a_{ij} < 0$) and the second many-body term a repulsive interaction ($b_{ij} > 0$). The weight functions $\omega_d(r_{ij})$, $\omega_C(r_{ij})$, and local density functions ($\bar{\rho}_i$) are described thoroughly in ref 5.

Published: February 14, 2012



Since the reduced units are commonly used in DPD simulations, we adopt in the rest of the paper the reduced units where r_c is the unit of length, $k_B T_0$ is the unit of energy with $T_0 = 298$ K, and m_{H_2O} the unit of mass. The correspondence between the DPD parameters in reduced units and the real values is given for completeness in Table 1.

Table 1. Correspondence Between the DPD Parameters in Reduced Units and the Real Values^a

DPD parameter	DPD → real units value	physical units value
bead	1	N_m 3 H ₂ O
r_c	1	$(\rho N_m V)^{1/3}$ 8.52 Å
ρ	6.88	$\rho N_m M / N_A r_c^3$ 997 kg m ³
γ	12.4	$\gamma k_B T / r_c^2$ 70.6 mN m ⁻¹
p	0.1	$p k_B T / r_c^3$ 0.67 MPa
a	50	$a k_B T / r_c$ 2.41×10^{-10} J m ⁻¹
α	0.101	α / r_c^4 5.32×10^{-38} m ⁴

^a r_c , ρ , γ , p , and a correspond to the cutoff radius, density, surface tension, pressure, and energy parameter, respectively. V is the volume of one water molecule (30 Å³), M the molar weight of a water molecule (18 g mol⁻¹), N_A is Avogadro's number, and k_B is Boltzmann's constant, T is 298 K. N_m is the number of water molecules in a DPD bead, and α is a parameter obtained by Groot and Warren²¹ to fit the DPD pressure.

To date no rigorous route allows a calculation of realistic MDPD parameters unlike the commonly used DPD method. Calculations of the DPD parameters are undertaken thanks to the FH theory.²⁰ Our MDPD parameters derivation is similar to the FH theory of polymers and can in fact be assimilated as a continuous version of this lattice model. In the FH theory, molecules of different length are confined in a lattice. The internal energy is described as a perturbation from ideal mixing where only the excess over pure components is taken into account. It has been shown that the repulsive crossed interaction term a_{ij} can be calculated²¹ from $a_{ij} = a_{ii} + 3.465\chi_{ij}$ with $\rho = 3$ and where $a_{ii} = a_{jj} > 0$ and χ_{ij} is the FH's parameter. This relation cannot be applied to the MDPD because it was only adjusted over the repulsive conservative energy parameters. In addition, MDPD is composed of an attractive and density dependent repulsive terms. These two features constitute the main restrictions to obtain realistic parameters for the MDPD method. Thus, one of the principal objectives of this work is to provide a route to develop MDPD parameters for realistic mesoscopic simulations.

For this, we begin to write the mean field (MF) MDPD pressure³ as $p_{\text{conf}}^{\text{MF}}/T = \rho + \alpha \rho^2 + 2\alpha \rho r_d^4(\rho^3 - c\rho + d)$, where ρ is the density, k_B the Boltzmann's constant, T the reduced temperature such that $T = T^{\text{real}}/T_0$, a and b the attractive and repulsive parameters, respectively, c and d are the constants, and $\alpha = 0.101$; α is a DPD parameter obtained by Groot and Warren²¹ and corresponding to a plateau of $(p - T\rho)/(\alpha\rho^2)$. The MF configurational pressure is given by

$$\frac{p_{\text{conf}}^{\text{MF}}}{T} = \alpha \rho^2 (a + 2br_d^4(\rho - c\rho^{-1} + d\rho^{-2})) \quad (2)$$

For a system of two components (A and B), the expression of the configurational pressure becomes

$$p_{\text{conf}} = \frac{1}{6V} \left[\sum_i \sum_{j \neq i}^{n_A} r_{ij} f_{ij} + 2 \sum_i \sum_j^{n_A} r_{ij} f_{ij} + \sum_i \sum_{j \neq i}^{n_B} r_{ij} f_{ij} \right]$$

where n_A and n_B are the particle numbers of A and B, respectively, r_i is the position vector of particle i , and f_{ij} the force between i and j . Thus, for two interacting types of particles we assume that $\rho_B = \rho_A = \rho$ (FH condition),²⁰ $\alpha_{AA} = \alpha_{BB} = \alpha$,²² $b_{AA} = b_{BB} = b$; b is kept constant in order to obtain a simple relation between the FH parameter and a . If b was a variable, then it would be impossible to express a simple relation between χ , a , and b . Therefore by keeping b constant, we simplify the problem that will allow us to use a simple relation to compute the attractive parameter from atomistic simulations. The cutoff r_c and r_d are identical for all of the interaction types. Then, based upon eq 3 the configurational part of $p_{\text{conf}}^{\text{MF}}$ becomes

$$\frac{p_{\text{conf}}^{\text{MF}}}{T} = \alpha \rho^2 (a_{AA}x^2 + 2a_{AB}x(1-x) + a_{BB}(1-x)^2) + 2b\alpha r_d^4(\rho^3 - c\rho + d) \quad (3)$$

where $x = (n_A/N)$ with $N = n_A + n_B$ leading $n_b = (1-x)N$ and $n_a = xN$. FH theory involves the knowledge of the free energy (F), such as $F = V\bar{f}$, where \bar{f} is free energy density. F is calculated from the pressure $p = -(\partial F/\partial V) = \rho^2(\partial/\partial\rho)(\bar{f}/\rho)$ so well that $(\partial/\partial\rho)[\bar{f}/\rho] = p/\rho^2$. By integrating eq 3 we find the configurational part of the free energy density

$$\frac{F_{\text{conf}}^{\text{MF}}}{T} = \alpha \rho^2 (a_{AA}x^2 + 2a_{AB}x(1-x) + a_{BB}(1-x)^2) + I\rho + 2b\alpha r_d^4 \left(\frac{\rho^3}{2} - c\rho \ln \rho - d \right) \quad (4)$$

where I is an integration constant. FH theory allows to link the mixing free energy (F^m) to the free energy of the pure component A ($x = 1$) and B ($x = 0$) $F^m = F^x - xF^1 - (1-x)F^0$. As $F = V\bar{f}$ we obtain $F_{\text{conf}}^m = 2\alpha N\rho T(a_{AB} - (a_{AA} + a_{BB}/2))x(1-x)$, where the term with b and I vanish. Identification with the configurational part of FH relation^{21,22} ($F_{\text{conf}}^m = NT\chi_{AB}x(1-x)$) allows us to obtain an expression of the FH mixing parameter χ_{AB}

$$\chi_{AB} = 2\alpha \rho \left(a_{AB} - \frac{a_{AA} + a_{BB}}{2} \right) \quad (5)$$

Using the classical FH theory, χ_{AB} can be calculated from

$$\chi_{AB} = \frac{Z_{ij}\langle U_{ij} \rangle + Z_{ji}\langle U_{ji} \rangle - (Z_{jj}\langle U_{jj} \rangle + Z_{ii}\langle U_{ii} \rangle)}{2} \quad (6)$$

where $\langle \dots \rangle$ is the average ensemble, $Z_{\alpha\beta}$ the coordination number of α , i.e., the nearest-neighbor of β around α , $U_{\alpha\beta}$ is the energy between α and β groups when α is surrounded by β . $U_{\alpha\beta}$ is calculated from separated molecular dynamic simulations by considering electrostatic and van der Waals interactions. Coordination numbers are evaluated from integrating the radial distribution functions. These results agree with the biased sampling calculation $U_{\alpha\beta}$ and $Z_{\alpha\beta}$.²² The cross parameters are

given by $a_{AB} = a_{AA} + (\chi_{AB}/2\alpha\rho)$. Thus we obtain a similar relation to DPD.^{21,22} Numerous Monte Carlo simulations were carried out in the NpT ensemble for several binary mixtures where only the crossed interaction (a_{ij}) was changed from -20 to -150 . Afterward we adjusted $2\alpha\rho(a_{AB} - a_{AA})$ from a linear fit to obtain eq 7. The adjustment is given in Supporting Information.

It is possible to use a quadratic adjustment, but this would be addressed in a future work on miscible mixture simulations. Equation 7 can be suitable to compute the interfacial tension of polymer blend with MDPD model. From the usual DPD method, eq 7 is not suitable, and the relation established by Groot and Warren²¹ must be used.

$$a_{AB} = a_{AA} + 0.606\chi_{AB} \quad (7)$$

■ COMPUTATIONAL PROCEDURE

The attractive parameters⁵ of salt and water are $a_{AA} = a_{BB} = -50$, while $b_{AA} = b_{BB} = b_{AB} = 25$. We take the same route as used by recent DPD simulations of polyelectrolytes^{23–25} and salt solutions.^{23,24,26} The electrostatic interactions are calculated using the Ewald summation method with charges distributed over the particles according to the method proposed by Gonzalez-Melchor et al.²³ Another strategy consists in using the particle–particle particle mesh technique adapted by Groot²⁶ to DPD models. It was established in a recent paper²⁴ that the two methods lead to the same mechanical and structural properties of different electrolyte systems.²⁴ As a result, we take the route of using the Ewald summation technique that allows a straightforward use of the Irving and Kirkwood definition²⁷ for the surface tension calculation.²⁴ The dielectric discontinuity is directly accounted for by considering the dielectric constant of water ($\epsilon_r = 80$). This approach is equivalent to the solvent primitive model (SPM),¹² where the solvent is implicitly model. However, in this work the solvent is explicitly accounted for using the many-body interactions. Thus, the interface is clearly defined and located in contrast to the SPM model where an additional force is introduced to explicitly consider the charge image effect. The range of the repulsive many-body interaction is fixed to $r_d = 0.75$. The equations of motions of the MDPD simulations are integrated using a modified velocity Verlet algorithm. The time step is $\delta t = 0.01$ and corresponds to a physical value of 6.8 ps (Table 1). The equilibration phase is formed by 5×10^5 steps, and the average thermodynamic properties are averaged over 10^6 additional steps in the constant NVT ensemble. The corresponding effective MDPD simulation time is about 7 μ s. The MDPD simulations use a simulation cell of 3072 DPD beads with $L_x = L_y = 7$ and $L_z = 50$. The corresponding real dimensions are $L_x = L_y \approx 60$ Å and $L_z = 426$ Å. The number of ions is calculated to match the real concentration (from 0.2 to 5.1 mol L⁻¹).^{24,23} The real concentrations have been calculated from $C^{\text{real}}(\text{salt}) = 10^4(\rho_{\text{salt}}N_m)/(6.023r_c^3)$, where $C^{\text{real}}(\text{salt})$ is the real concentration and ρ_{salt} is the DPD density of salt. The physical length scale of MDPD is related to the density of bulk liquid phase. Indeed, as $r_c^3 = \rho V_{\text{H}_2\text{O}}N_m$, where $V_{\text{H}_2\text{O}}$ is the volume of one water molecule (≈ 30 Å³) and N_m is the number of water molecules belonging to one MDPD bead ($N_m = 3$).

From the molar volume of Na⁺, F⁻, and Cl⁻ we deduce that one DPD cation and anion bead represents three real ions. Therefore this calculation dictated by the volume molar is not ‘ad-hoc’. The real concentrations are calculated accounting this description. By taking the same number of cations and anions,

the electroneutrality is conserved. In addition, from the atomistic radial distribution functions of Na⁺–Na⁺ and Cl⁻–Cl⁻ we check the possibility to form a cluster of three ions. Indeed, we find an ion–ion contact distance of 4.3 Å. At this distance, repulsive electrostatic and dispersive interactions are equilibrated. Thus, in the following section, our discussion will concern the MDPD bead of water, Na⁺ and Cl⁻. Atomistic simulations have been carried out in the NpT statistical ensemble using the TIP4P/2005 water model²⁸ and the recent Reif’s model for NaCl and NaF²⁹ at $T = 298$ K and $p = 1$ bar. Liquid–vapor interface is modeled from the usual atomistic procedure.³⁰ We opt for these ions for their weak polarizability (α). Indeed, consideration of α in MDPD would require additional developments which are outside the scope of this work. The MDPD interaction parameters sets are given in Table 2. Results are given in real units using the relations

Table 2. Different Sets of MDPD Parameters^a

Set 1				
	Na ⁺	Cl ⁻	W	q
NaCl				
Na ⁺	-50.0	-50.0	-73.8	+3
Cl ⁻	-50.0	-50.0	-73.9	-3
W	-73.8	-73.9	-50.0	0
Set 1				
	Na ⁺	F ⁻	W	q
NaF				
Na ⁺	-50.0	-50.0	-79.0	+3
F ⁻	-50.0	-50.0	-80.5	-3
W	-79.0	-80.5	-50.0	0
Set 2				
	Na ⁺	Cl ⁻	W	q
NaCl				
Na ⁺	-50.0	-65.4	-73.8	0
Cl ⁻	-65.4	-50.0	-73.9	0
W	-73.8	-73.9	-50.0	0

^aAttractive parameter a_{ii} between two identical species is kept to -50 and with $b_{ii} = b_{ij} = 25$. The set 0 model is defined by fixing the a_{ij} parameters to -50 , a positive charge (+3) for Na⁺ and a negative charge (-3) for Cl⁻. The W symbol refers to water and q to the partial charge of the coarse grained particles.

defined in ref 5. For MDPD and MD simulations mechanical and thermal equilibrium have been checked.

■ RESULTS AND DISCUSSION

Within the set of parameters (set 1), salt and solvent particles have the same parameters ($a_{ii} = -50$). The cross-interactions a_{ij} between the salt and the water are calculated from the FH parameters, whereas the unlike interactions between Na⁺ and Cl⁻ are kept to -50 . In the standard DPD simulations, the water–salt cross-interactions a_{ij} are the same as a_{ii} leading to a deficient modeling of the ions’s hydration. However, Levin and Flores-Mena³¹ have clearly shown that the hydration of ions prevents the centers of ions from coming closer than $a/2$ to the GDS (a is diameter of ions) and contributes to the understanding of the increase of surface tension. Figure 1a shows that the surface tension of the classical charged DPD model (set 0 in Table 2) does not increase with the salt concentration. This suggests that the combination of electrostatics with standard MDPD parameters is not able to

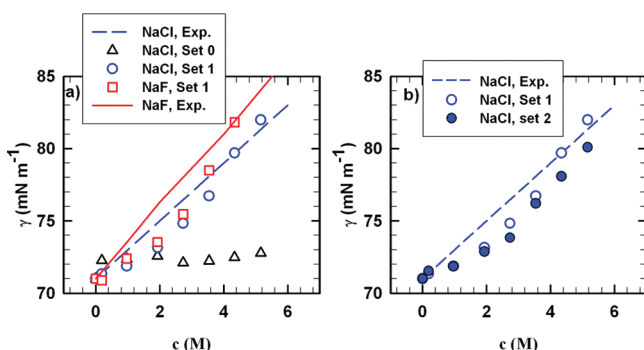


Figure 1. Surface tension of water as a function of the salt concentration for different models indicated in the insets: (a) for NaCl and NaF solutions and (b) for NaCl at low concentrations and for NaCl solution for the set 1 and set 2 models.

reproduce the dependence of the surface tension on the salt concentration, making the charge image concept no longer valid at the mesoscopic scale and high concentration. It is worth pointing out that the screening length is 9.7 Å for a 1:1 electrolyte at 0.1 M concentration in water, falling (as $1/\sqrt{c}$) to 3.0 Å at 1 M concentration and so on. So for all the simulation points of Figure 1, the screening length is less than the decay length λ of the Slater-type charge density²³ ($\lambda = 9.1$ Å). The physical behavior takes place on a length scale which is not properly resolved by the mesoscale model. It is not surprising that the concentration dependence of surface tension is not reproduced with the set 0 for the higher concentrations. At these ionic strengths, <0.1 M, the screening length is also of the same order of magnitude as the hydrated ion size. Hence one might expect that an accurate model of the interaction between hydrated ions and the interface is warranted. Therefore, as shown in Figure 1b, it seems that the electrostatic interaction in MDPD and DPD is sufficient for biophysical applications (≤ 0.1 M salt). With the concentration >0.1 M, we can neglect electrostatics interactions and introduce a short-range repulsion (set 2). The ions are excluded from the interface boundary by the distance equal to the size of the hydrated ion. This is essentially in accordance with the findings of Levin and co-workers.^{9,31}

Thus, we consider the specific interactions between water and salt to accurately describe the hydration effect. Our approach amounts to considering the total energy of atomistic simulation (electrostatic and van der Waals contributions) to calculate the FH parameters. To investigate the impact of the electrostatics, we test two models: one with electrostatic charges (set 1) and a second model without any charges (set 2). In the set 2 model, the interaction parameters between Na⁺ and Cl⁻ are explicitly calculated from the FH parameter unlike the set 1 model.

Figure 1a,b shows that the set 1 and 2 models reproduce the surface tension of the liquid–vapor interface of electrolytic solutions. In addition, the dependence of the surface tension with the salt concentration is also very well predicted. We also reproduce the specificity of inorganic salt in terms of surface tension. From an atomistic point of view, the situation differs because the physical ingredients at the microscopic scale, as hydrogen bonding and polarizability are not accounted for in coarse grained simulations. Indeed, DPD simulation is a coarse grained method, which leads to some atomistic details that are sacrificed. As a consequence, it becomes difficult to capture specific molecular interactions, such as hydrogen bonds.

Nevertheless, thermodynamic and interfacial properties are well reproduced due to the derivation of DPD parameters from atomistic simulations. Actually, this work is a first attempt to derive a DPD parameters to describe the liquid–vapor interface of the electrolytes. Additional developments are required to really account for the whole of physics (such as the polarizability). However, it is possible to predict the macroscopic properties as surface tension from a multiscale modeling and an effective potential. Figure 1c shows that the two models predict very well the salt dependence of the surface tension, indicating that the use of explicit electrostatic interactions is not required in MDPD simulations, on condition that all the cross-interactions are considered in the multiscale adjustment procedure. It does not involve that the electrostatic interactions do not play a role in the underlying interfacial physics. Indeed, the electrostatic interactions between water and ions have been embedded in the DPD parameters. Therefore the electrostatic interactions between ions and water are not directly quantifiable from DPD simulations. We have only investigated the role of the electrostatic interactions between Na⁺ and Cl⁻ and concluded to the weak influence of this Coulombic pairwise interaction on the surface tension.

We now focus on the origin of the increase of the surface tension. We report in Figure 2 the radial distribution function

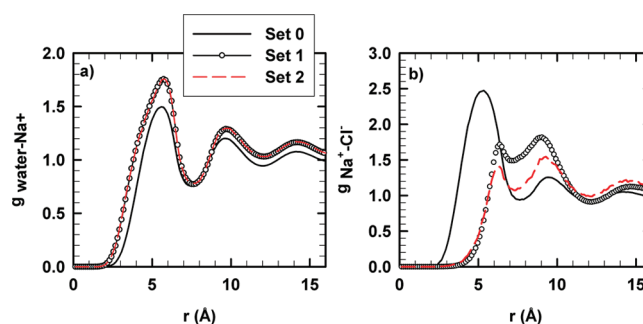


Figure 2. Radial distribution functions between (a) water and Na⁺ and (b) Na⁺ and Cl⁻ for different sets of parameters.

between coarse grained water and Na⁺ and between Na⁺ and Cl⁻. We specify that the radial distribution functions are not interpreted in terms of ion–ion distance because one DPD bead corresponds to three real ions. Figure 2 shows similar distribution functions with the set 1 and 2 models indicating that the structural properties of the salt solutions are similarly reproduced in line with the similar prediction of the surface tension. In addition, the set 0 parameters and the other models lead to significant differences in the Na⁺ – Cl⁻ distributions (Figure 2b). Indeed, from the sets 1 and 2, the hydration first shell is more hydrated in comparison to the set 0. This leads to an increase of the number water molecules located between Na⁺ and Cl⁻ that impacts the distribution function between Na⁺ and Cl⁻. Figure 2a depicts the raise of the coordination number from the increase of the intensity of distributions. With the set 1 and 2 models, the position of the peaks is similar with only slight differences in the coordination number of the two first shells. Results indicate that modeling of the mesoscopic ions hydration leads to a good reproduction of the surface tension dependence with the salt concentration.³¹

One aspect of the theory of Y. Levin and J.E. Flores-Mena is a depletion boundary related to the free-ion layer concept. This specific behavior of ions at the water surface shown in Figure 3

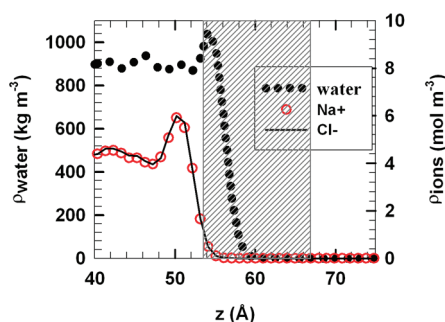


Figure 3. Density profiles of water, cation, and anion along the z -axis. The free-ion layer is represented in gray to show the ion depletion zone between 52 and 60 Å.

is then taken into account by our mesoscopic models. In contrast to polarizable and nonpolarizable molecular simulations^{11,16} and theory,^{8,9} the cation and anion present different density profiles. For Na^+ and Cl^- we obtain similar profiles given that the DPD interactions parameters between water and ions are almost the same (73.9 for Na^+ and 73.8 for Cl^-). Furthermore, the DPD water beads are uncharged leading to that the soft potential plays an important role. With an unpolarizable molecular simulation, D. Bhatt and co-workers¹² report similar density profiles between Na^+ and Cl^- . This clearly suggests a force field dependence. Discrimination between two ions can be possible if we refine the derivation procedure. However, the main objective of this study was to develop a DPD method to compute the interfacial properties. Whereas the DPD model used here cannot describe microscopic details below the physical length of 8.5 Å, it allows the calculation of macroscopic properties over larger time and length scales.

CONCLUDING REMARKS

We have shown that the interfacial properties of salt solutions can be predicted from many-body DPD simulations using the FH theory, although some atomistic details are missing in the coarse graining model. The resulting parameters reproduce the increase of surface tension with the salt concentration and the specificity of inorganic salt at the water–air interface. The values of the surface tension are also in line with the experimental ones. The charge image concept is not the only criteria to explain the dependence of the surface tension on salt concentration at a mesoscopic scale. The physical key property is the hydration effect of salts. Our mesoscale modeling is in agreement with the theory suggesting a free-ion layer at the interfacial boundary. Therefore, this work opens the way of the realistic many-body DPD simulations of interfacial properties of multicomponent mixtures.

ASSOCIATED CONTENT

Supporting Information

This material is available free of charge via the Internet at <http://pubs.acs.org>.

AUTHOR INFORMATION

Corresponding Author

*E-mail: Aziz.Ghoufi@univ-rennes1.fr.

Notes

The authors declare no competing financial interest.

ACKNOWLEDGMENTS

A.G. thanks David Bouchet for the careful reading of the manuscript.

REFERENCES

- (1) Hoogerbrugge, P. J.; Koelman, J. M. V. A. *Europhys. Lett.* **1992**, *19*, 155.
- (2) Pagonabarraga, I.; Frenkel, D. *J. Chem. Phys.* **2001**, *115*, 5015.
- (3) Warren, P. B. *Phys. Rev. E* **2003**, *68*, 066702.
- (4) Ghoufi, A.; Malfreyt, P. *Phys. Rev. E* **2010**, *82*, 016706.
- (5) Ghoufi, A.; Malfreyt, P. *Phys. Rev. E* **2011**, *83*, 051601.
- (6) Arienti, M.; Pan, W.; Li, X.; Karniadakis, G. J. *J. Chem. Phys.* **2011**, *134*, 204114.
- (7) Heydweiller, A. *Ann. Phys. (Leipzig)* **1910**, *33*, 145.
- (8) Levin, Y.; dos Santos, A. P.; Diehl, A. *Phys. Rev. Lett.* **2009**, *103*, 257802.
- (9) Levin, Y. *Phys. Rev. Lett.* **2009**, *102*, 147803.
- (10) Jungwirth, P.; Tobias, D. J. *J. Phys. Chem. B* **2001**, *105*, 10468.
- (11) D'auria, R.; Tobias, D. J. *J. Phys. Chem. A* **2009**, *115*, 7286.
- (12) Bhatt, D.; Newman, J.; Radke, C. J. *J. Phys. Chem. B* **2004**, *108*, 9077.
- (13) Frumkin, A. Z. *Phys. Chem.* **1924**, 109.
- (14) Markovich, G.; Pollack, S.; Giniger, R.; Cheshnovsky, O. *J. Chem. Phys.* **1991**, *95*, 9416.
- (15) Ghosal, S. *Science* **2005**, *307*, 567.
- (16) Garret, B. *Science* **2004**, *303*, 1146.
- (17) Onsager, L.; Samaras, N. N. T. *J. Chem. Phys.* **1934**, *2*, 258.
- (18) Trofimov, S. Y.; Nies, E. L. F.; Michels, M. A. J. *J. Chem. Phys.* **2002**, *117*, 9383.
- (19) Trofimov, S. Y.; Nies, E. L. F.; Michels, M. A. J. *J. Chem. Phys.* **2005**, *123*, 144102.
- (20) Flory, P. *Principles of Polymer Chemistry*; Cornell University Press: Ithaca, NY, 2011; p 12.
- (21) Groot, R. D.; Warren, P. B. *J. Chem. Phys.* **1997**, *107*, 4423.
- (22) Ryjkina, E.; Kuhn, H.; Rehage, H.; Muller, F.; Peggau, J. *Angew. Chem., Int. Ed.* **2002**, *41*, 983.
- (23) Gonzalez-Melchor, M.; Mayoral, E.; Velazquez, M. E.; Alejandro, J. J. *J. Chem. Phys.* **2006**, *125*, 224107.
- (24) Ibergay, C.; Malfreyt, P.; Tildesley, D. J. *J. Chem. Theory Comput.* **2009**, *5*, 3245.
- (25) Ibergay, C.; Malfreyt, P.; Tildesley, D. J. *J. Phys. Chem. B* **2010**, *114*, 7274.
- (26) Groot, R. D. *J. Chem. Phys.* **2003**, *118*, 11265.
- (27) Irving, J. H.; Kirkwood, J. G. *J. Chem. Phys.* **1950**, *18*, 817.
- (28) Abascal, J. L. F.; Vega, C. *J. Chem. Phys.* **2005**, *123*, 234505.
- (29) Reif, M. M.; Hünenberger, P. H. *J. Chem. Phys.* **2011**, *134*, 144104.
- (30) Ghoufi, A.; Goujon, F.; Lachet, V.; Malfreyt, P. *J. Chem. Phys.* **2008**, *128*, 154716.
- (31) Levin, Y.; Flores-Mena, J. E. *Europhys. Lett.* **2001**, *56*, 187.